

Wind turbine performance enhancement with minimal structural load penalty: A design philosophy

Wind Engineering

1–17

© The Author(s) 2024

Article reuse guidelines:

sagepub.com/journals-permissions

DOI: 10.1177/0309524X231212565

journals.sagepub.com/home/wieVijay Matheswaran¹  and Patrick J Moriarty²

Abstract

The performance benefits of using tip devices on wind turbines has been well-documented. However, previous studies show that adding blade tip devices such as winglets leads to a significant increase in blade root bending moment, potentially requiring structural reinforcement with cost and weight drawbacks. A new and unique design philosophy for retrofit blade tip devices for wind turbines is presented. By balancing generated aerodynamic and centrifugal loads, these devices offer an increase in power production without the need for structural reinforcement. Predicted performance and cost benefits of using retrofit blade tip devices on the National Renewable Energy Laboratory 5 MW reference wind turbine are shown. The addition of blade tip devices resulted in significant improvements in the coefficient of power (C_p) and annual energy production (AEP).

Keywords

Wind energy, blade tip devices, vortex lattice method, wind turbine design, power production

Introduction

A driving parameter in the wind industry is the cost of energy (COE), usually measured in \$/KWh. There has been a concentrated effort by the industry and research community to bring down the COE, allowing wind to be more competitive with other sources of energy. A logical approach to driving down the COE is to improve the annual energy production (AEP) of a wind turbine. While new wind turbines are routinely being designed with larger rotor diameters to increase the amount of energy captured from the wind, a second approach is to use blade tip devices to improve the efficiency of the thousands of older wind turbines already in operation. Blade tip devices are attractive as they offer performance increments without increasing rotor span and projected area. However, using blade tip devices does typically have the drawback of increased root bending moments and thrust on the rotor.

Gyatt and Lissamann (1985) did the earliest studies on using blade tip devices to improve aerodynamic efficiency. They employed four tip designs on a 25 kW Carter wind turbine in San Geronio, California. These designs were based on wing tip shapes being used in aircraft to reduce drag. The authors compared the results to analytical results from Wilson and Lissamann's PROP code. They found that tip devices did not offer meaningful improvements in power produced as predicted. However, this was attributed to the limited modeling tools available to the authors at that point. Subsequent studies did show that significant improvements in power can be obtained through the use of blade tip devices such as winglets. These tip devices were usually designed using free-wake lifting line (FWLL) or vortex lattice methods (VLM). Imamura et al. (1998) analyzed the effect of winglets on wind turbines using a free wake vortex lattice method, comparing winglets with varying cant angles to a simple span extension. They showed that winglets did offer a similar increase in power produced as a span extension, but with a smaller increment in root bending moment. Gaunaa and Johansen (2008, 2007) modeled a theoretical rotor

¹Department of Aerospace Engineering, Wichita State University, Wichita, KS, USA

²Wind Energy Systems Group, National Renewable Energy Laboratory, Golden, CO, USA

Corresponding author:

Vijay Matheswaran, Department of Aerospace Engineering, Wichita State University, 1845 Fairmount, Wichita, KS 67260, USA.

Email: vijay.matheswaran@wichita.edu

with a diameter of 126 m, and designed a downwind winglet by optimizing circulation on the rotor using a FWLL model and a gradient algorithm. They found that the FWLL predicted a 2.47% increase in the coefficient of power C_p when using a 2% downwind winglet, while CFD results from Ellipsys 3D led to an increase in C_p of 1.74%. The same study showed, using a vortex tube model, that the benefits from winglets were due to the reduction of tip losses and allowing the loading on the rotor to be extended on to the winglet. Then, there is an increase in bound circulation on the blade, leading to higher power production. The authors also showed that downwind winglets were found to be more efficient. When upwind winglets are used, the shed vorticity reduces axial velocities and thus power production on the main rotor. Downwind winglets bring the trailing vorticity downstream and out of the rotor plane.

Later studies adopted a parametric approach to blade tip device design using both numerical and experimental tools. Johansen et al. (2008) studied the effects of a vertical winglet and described the main design parameters involved in winglet design for a wind turbine. They showed that sweeping the winglet and adding tip twist did not significantly affect the mechanical power output of the wind turbine. Radius of curvature and winglet height were two parameters that affected the power produced. Maniaci and Maughmer (2012) designed winglets for a model-scale turbine using a free-wake vortex lattice method, and predicted peak increase in C_p of over 10%. Experimental results showed a peak increase of 9.1% for a narrow range of operating conditions, which dropped to a gain of 4% for a broad range of tip-speed ratios. In Hansen and Mühle (2018), an optimization process for winglet design is presented. The optimized winglet increased power for a model-scale turbine by 7.8%. Zhu et al. (2017) studied the effectiveness of upwind, downwind, and split winglets. They found that winglets bent to the pressure side were slightly more efficient than those bent to the suction side, but state that best performance is achieved when the angle of the winglet is aligned with the angle of the inflow. Tobin et al. (2015) compared the performance of a rotor with and without winglets, and noted an increase in both C_p and thrust with the use of winglets.

The benefits of using blade tip devices have been clearly demonstrated in literature, but they are not without drawbacks. In attempting to design blade tip devices that offer maximum efficiency (Elfarra et al., 2014; Hansen and Mühle, 2018), only the optimal aerodynamic solution is often considered. The addition of large blade tip devices designed to maximize aerodynamic load can lead to significant increase in blade root bending moment. Work done so far that analyzes the effects of blade tip devices while also quantifying the increase in blade root bending moment has been fairly limited. Imamura et al. (1998) noted that a winglet with a cant angle of 80° and height of 10% of rotor radius led to a 10% increase in blade root flapwise bending moment. Johansen et al. (2008) also noted that a loads analysis is necessary when studying the effect of blade tip devices.

Only recently has there been a focus on the idea of load-neutral or load-limited blade tip devices—that is, constraining the increase in loads on the baseline blade due to the addition of blade tip devices. Apart from previous related work by Matheswaran et al. (2019), only a few other studies have focused on load-neutral blade tip devices. Zahle et al. (2018) used a surrogate model to design optimized tip shapes for the International Energy Agency 10 MW reference turbine while constraining the flapwise bending moment at 90% radius. Similarly, Barlas et al. (2021) also used a surrogate model, but included full aeroelastic simulations when designing load-neutral tip extensions. Madsen et al. (2021) used a high-fidelity shape optimization framework and considered 12 design variables to optimize blade tip shape, with heavy focus on the CFD methodology. Considering only aerodynamic loads, they constrain increases in bending moment at 90% blade radius, leading to tip shapes that offer an increase in power. While the end objective is the same, the approach adopted in those three studies is fundamentally different from what is proposed here.

In this study, building on prior work (Matheswaran et al., 2019) that has been patented through Wichita State University (Miller and Matheswaran, 2019), the authors present a unique design philosophy for retrofit blade tip devices in wind turbines. The approach allows the use of retrofit blade tip devices that offer a meaningful increase in power production while keeping the increase in root bending moments to a minimum by balancing loads. In the subsequent sections, the design philosophy and tools used are explained, followed by results outlining the effects of retrofit blade tip devices on power produced and blade loads throughout the operational envelope of the wind turbine considered.

Design philosophy

The key differentiator between this study and prior work of others is the underlying design philosophy of designing a blade tip device that offers a meaningful increase in C_p with minimal increase in blade root bending moment. This is done by balancing the generated aerodynamic and centrifugal force on the blade tip device. Balancing forces allows the device to be light, thereby minimizing blade root bending moment and removing any need for

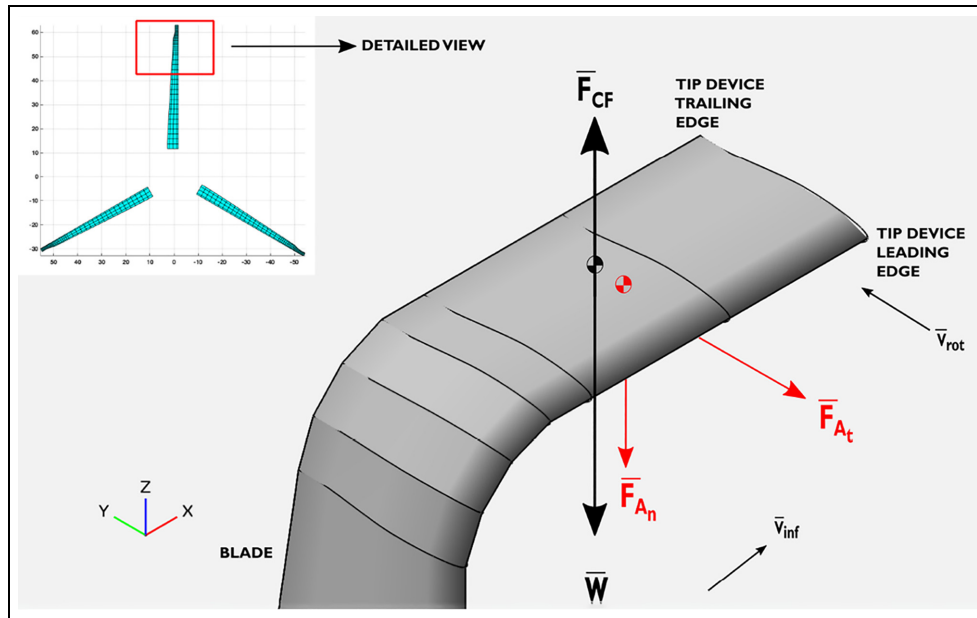


Figure 1. Freebody diagram of the blade tip device. Here, F_{CF} is the centrifugal force, W is the weight, and F_{A_n} and F_{A_t} are normal and tangential components of the aerodynamic force.

significant structural reinforcement. A lighter blade tip device also implies a cheaper and more cost-effective one. The addition of such balanced blade tip devices then offers reduction in tip losses, but without the increase in root bending moments typically associated with other blade tip devices. Accordingly, the best blade tip device is not one that offers maximum increase in C_p , but rather offers *an* increase in C_p while ensuring forces are balanced to within a threshold.

A freebody diagram of the blade with blade tip device is shown in Figure 1, whereas in Figure 2, a qualitative view of the design philosophy and the optimal design space is shown. Although similar in appearance to winglets, the authors have refrained from labeling these blade tip devices as winglets due to the difference in function. Traditionally, wind turbine winglets are designed to be highly loaded, allowing outer radial positions of the rotor to run with increased bound circulation (Gaunaa and Johansen, 2007). In this study, loading is extended onto the blade tip devices as well, but while ensuring the forces on the blade tip are balanced. This naturally minimizes any increase in blade root bending moments. Thus, this approach allows blade tip devices that allow *a meaningful* increase in C_p without significantly increasing blade root bending moment.

Methods

The NREL 5 MW reference turbine (Jonkman et al., 2009) was used as the baseline turbine in this study, and changes due to the addition of blade tip devices are compared to the baseline case. To gauge the efficacy of blade tip devices developed using the design philosophy, a VLM with a prescribed wake is used. Blade element momentum theory (BEMT), although fast and widely used in the wind industry, uses corrections to account for three-dimensional tip effects, making it unsuitable to study the effects of blade tip devices on wind turbines (Schmitz and Maniaci, 2017). The VLM implemented here is based on theory presented in Katz and Plotkin (1991). The obtained results are compared with Abedi et al. (2013) and QBlade (Marten et al., 2013). A detailed overview of the VLM used in this paper is also presented in Matheswaran (2016).

To calculate the annual energy production (AEP) for the baseline case as well as the case with blade tips, it has been assumed that the baseline wind turbine is located in Wichita, Kansas. Wind speed data for Wichita (Jong and Thoman, 1978), measured at a height of 25 feet, is used, with shape and scale factors scaled to the hub height of the NREL 5 MW reference turbine. The power curve for the NREL 5 MW is constructed using the approximate cubic power curve method outlined in Carrillo et al. (2013). A cost model is used to calculate levelized cost of energy (LCOE) for the baseline turbine and the turbine with blade tip devices.

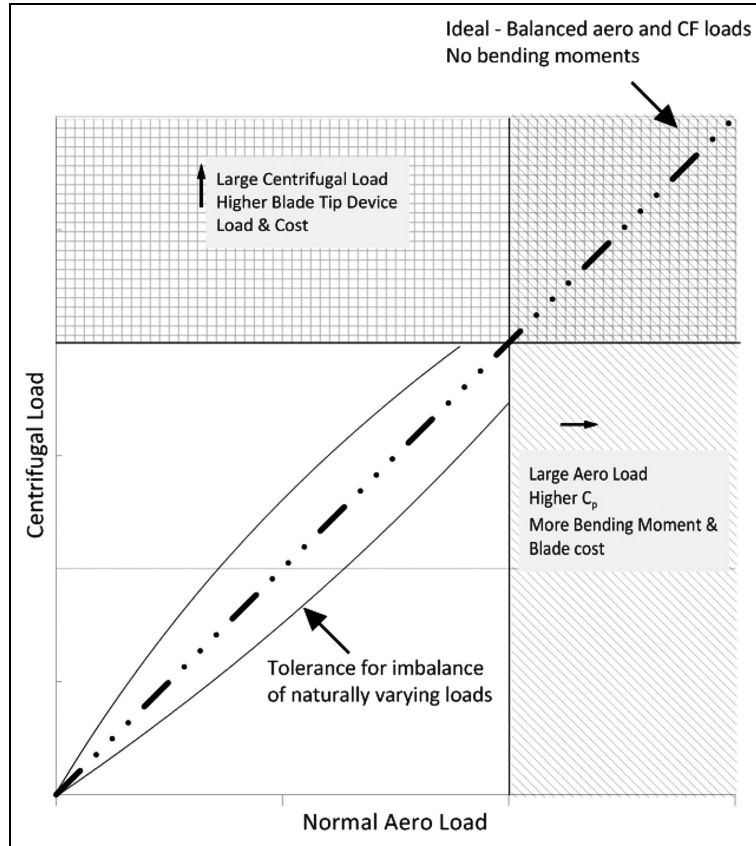


Figure 2. Design space for blade tip devices.

Vortex lattice method

Jonkman et al. (2009) provide structural and aerodynamic properties of the NREL 5 MW reference turbine. These properties are used to model the turbine in OpenVSP (McDonald and Gloudemans, 2022), a parametric geometry modeling tool. The blade camber surface is discretized into discrete panels along the span and chord. A vortex ring of strength Γ is overlaid on each panel, representing it as a surface of vorticity. The velocity induced by each vortex filament is given by the Biot-Savart Law, represented in Katz and Plotkin (1991) as:

$$v_{ind} = \frac{\Gamma}{4\pi} \frac{r_1 \times r_2}{|r_1 \times r_2|} \frac{r_o}{r_1} \frac{r_2}{r_2} \quad (1) \leftarrow$$

Here, Γ is the strength of the vortex element, r_1 and r_2 are position vectors from an arbitrary point P to the start and end points of the vortex filament respectively. The term r_o is defined as

$$r_o = r_2 - r_1 \quad (2) \leftarrow$$

If the point P is located on the vortex filament, the Biot-Savart Law is singular. Additionally, when r_1 and r_2 are collinear, the formulation above is indeterminate even if the point of evaluation lies outside the vortex filament. To address this, Phillips and Snyder (2000) suggest an adaptation as:

$$v_{ind} = \frac{\Gamma}{4\pi} \frac{(r_1 \times r_2)(r_1 + r_2)}{r_1 r_2 (r_1 r_2 + r_1 \cdot r_2)} \quad (3) \leftarrow$$

When the evaluation point is very close to the vortex filament, extremely large induced velocities result. To account for this, a cut-off radius δ is used:

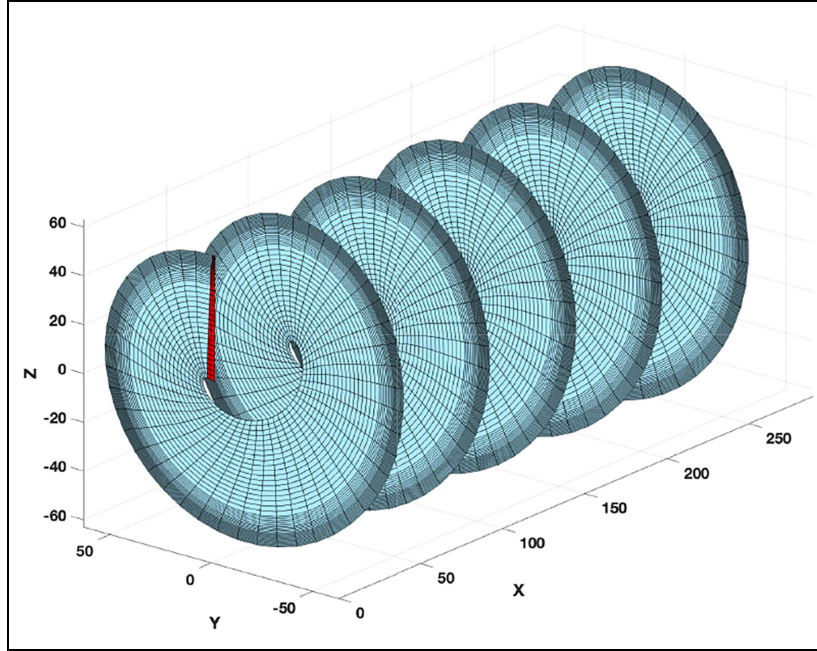


Figure 3. Vortex lattice prescribed wake for a single blade.

$$v_{ind} = \frac{\Gamma}{4\pi} \frac{(r_1 \times r_2)(r_1 + r_2)}{r_1 r_2 (r_1 r_2 + r_1 \cdot r_2) + (\delta r_o)^2} \quad (4) \leftarrow$$

The value of δ used in the implemented vortex lattice method is 0.1.

This formulation of the Biot-Savart law allows representing the blade as a surface of vorticity and calculation of rotor-induced velocity at the rotor plane. The two-dimensional Kutta condition is satisfied by placing the leading segment of each vortex ring at the quarter-chord line of each panel (Katz and Plotkin, 1991). In this study, each blade is divided into 4 chordwise panels and 43 spanwise panels. Because circulation gradients close to the tip of the blade can be large, the concentration of panels is increased there. Van Garrel (2003) recommends the use of cosine grid spacing.

Having set up the geometry, the wake behind the wind turbine is generated. A free-wake, while more accurate, is computationally demanding (Kecskemety and McNamara, 2011). In this study, a prescribed wake is used as the objective is to capture trends in differences between wind turbines with and without blade tip devices. The initial wake geometry is described as a helix (Abedi et al. (2013)):

$$x = v_{\infty} t \quad (5) \leftarrow$$

$$y = r_i \sin(\Omega t + \theta_t) \quad (6) \leftarrow$$

$$z = r_i \cos(\Omega t + \theta_t) \quad (7) \leftarrow$$

Here, v_{∞} is the freestream velocity in m/s, r_i is the blade section radius in m, Ω is the blade rotational velocity in rad/s and θ_t is the blade section twist in radian. The wake is allowed to extend five diameters downstream of the turbine. The velocity induced by a wake panel five diameters downstream on the first blade panel is of the order of 10^{-6} m/s. As this is close to negligible, the wake is truncated here. Extending wake filaments to infinity (as is expected in an incompressible, inviscid, and irrotational model) is both unrealistic and inefficient. The blade geometry and prescribed wake behind one blade is shown in Figure 3. Collocation or control points are located at the three-quarter chord point of each blade panel, which is the midpoint of each vortex ring. The normal vector at each control point can now be calculated.

To calculate blade bound circulation, the flow tangency boundary condition (zero normal flow across the boundary) is applied:

$$(v_\infty + v_{ind, bound} + v_{ind, wake} + v_{rot}).n = 0 \quad (8) \leftarrow$$

Here, $v_{rot} = \Omega \times r$. Induced velocities due to blade bound vortices and trailing wake vortices are calculated using the Biot-Savart Law. To initialize a solution, a value of $\Gamma = 1 \text{ m}^2/s$ is used. It is now possible to shift the normal components of the known velocity to the right-hand side of equation (8). An influence coefficient $a_{i,j}$ can be defined at each control point. It is the sum of the normal induced velocities (both bound and trailing wake) by a vortex ring of strength ($\Gamma = 1$) at each collocation point. So $a_{i,j}$ is the influence of the j^{th} vortex ring on the i^{th} blade collocation point and is written as:

$$a_{i,j} = v_{i,j,ind,bound} + v_{i,j,ind,trailingwake} .n \quad (9)$$

A system of equations are constructed as below:

$$\begin{pmatrix} a_{1,1} & & a_{1,N} \\ \vdots & \ddots & \vdots \\ a_{N,1} & & a_{N,N} \end{pmatrix} \begin{pmatrix} \Gamma_1 \\ \vdots \\ \Gamma_N \end{pmatrix} = \begin{pmatrix} (v_\infty + \Omega \times r).n_1 \\ \vdots \\ (v_\infty + \Omega \times r).n_N \end{pmatrix} \quad (10) \leftarrow$$

The Kutta condition ($\gamma = 0$) is specified by setting the strength of the trailing vortex rings equal to the blade vortex ring at the trailing edge (Katz and Plotkin, 1991)). Because the strength of the vortex panels do not change with time, they can be converted into trailing horseshoe vortices. The effect of each trailing wake vortex is added to the last chordwise panel of each spanwise segment. Circulation values across each blade can now be calculated. Using this approach, correct induced velocities can be determined. The geometric angle of attack at each blade section is calculated as:

$$\alpha_{geom} = \tan^{-1} \frac{v_n}{v_t} \quad (11) \leftarrow$$

The term v_n here is the sum of the rotational and freestream velocity normal to the blade, v_t is the sum of the rotational and freestream velocity tangent to the blade. Induced velocities by the trailing wake leads to a reduction in the angle of attack. Then, the effective angle of attack is:

$$\alpha_{eff} = \tan^{-1} \frac{v_{totn}}{v_{tott}} \quad (12) \leftarrow$$

Here, v_{totn} and v_{tott} are the total velocity components that are normal and tangential to the blade, respectively. The effective angle of attack is used to compute section lift and drag coefficients by using two-dimensional airfoil data. Using two-dimensional airfoil data allows the quantifying of viscous effects in this inviscid model. Computed forces are broken down in the normal and tangential direction, and used to calculate power generated by the turbine.

The VLM model implemented in this study is validated by comparing generated results to published results in Jonkman et al. (2009) and to simulations from QBlade. These results are presented in Table 1. All comparisons are done at a wind speed of 8 m/s and a tip speed ratio of 7.55, because these are the operating conditions that lead to maximum C_p for the NREL 5 MW turbine. Circulation and induced angle of attack distributions are also compared with Abedi et al. (2013), with $v_\infty = 8 \text{ m/s}$ and $\Omega = 1.0032 \text{ rad/s}$ used as the operating conditions. Abedi et al. (2013) do not present specific details on how the turbine was modeled, but it can be seen that the results compare well to results from the VLM implemented here. The angle of attack distribution and circulation distribution across the blade radius is presented in Figures 4 and 5 respectively.

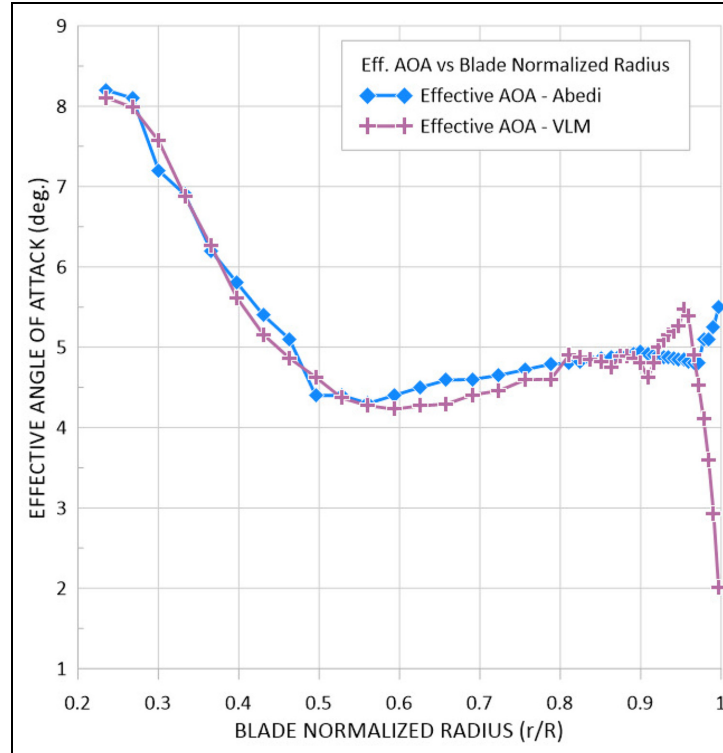
It must be noted that the objective of the VLM used in this study is not to recreate exact results from QBlade (Marten et al., 2013) or Jonkman et al. (2009), but rather to have a tool that is capable of capturing and quantifying differences produced if the new blade tip devices are used on wind turbines. The results show that the implemented VLM is capable of doing so.

Economic Model

To determine any change in the LCOE due to the use of blade tip devices, it is essential to arrive at a baseline cost for the NREL 5 MW reference turbine. Because Jonkman et al. (2009) do not provide cost estimates for the

Table 1. Comparison of results using different methods. Test conditions are $V_\infty = 8\text{m/s}$ and $\text{TSR} = 7.55$.

Model	Power (kW)	C_p
QBlade lifting line model, Marten et al. (2013)	2087	0.5340
Vortex lattice method	2007	0.5134
NREL 5 MW reference, Jonkman et al. (2009)	1884	0.4820

**Figure 4.** Effective angle of attack distribution along blade span. Results from the implemented VLM are compared to Abedi et al. (2013).

NREL 5 MW reference turbine, cost scaling factors available in Fingersh et al. (2006) are used. These values are scaled up from 2002 dollars to 2016 dollars using data from the US Bureau of Labor Statistics (2016).

The LCOE model used is:

$$LCOE = \frac{I_t + M_t}{E_t} \quad (13)$$

LCOE is a $\$/\text{kWh}$ value. I_t here is the initial cost per year, M_t is the annual operating expense, and E_t is the annual energy production (AEP). The initial cost includes capital cost and fixed charge rate (FCR), extended over the life-span of the wind turbine. FCR here is set at 11.58%, as per Fingersh et al. (2006), and lifespan is set at 20 years as is the industry trend.

The annual operating expense includes the cost of operations and maintenance of the wind turbine. It includes the operation and maintenance (O&M) Costs, land lease costs (LLC) and the levelized replacement costs (LRC). Using the cost scaling factors for each in Fingersh et al. (2006), the total annual operating expense is calculated. Annual operating expense for the NREL 5 MW reference turbine is shown in Table 2.

The AEP is the value of the net energy produced by the wind turbine measured in kWh. As stated earlier, it has been assumed that the baseline wind turbine is located in Wichita, Kansas. Jong and Thoman (1978) have documented Weibull probability distribution, and shape and scale factors for wind speed data measured at a height of

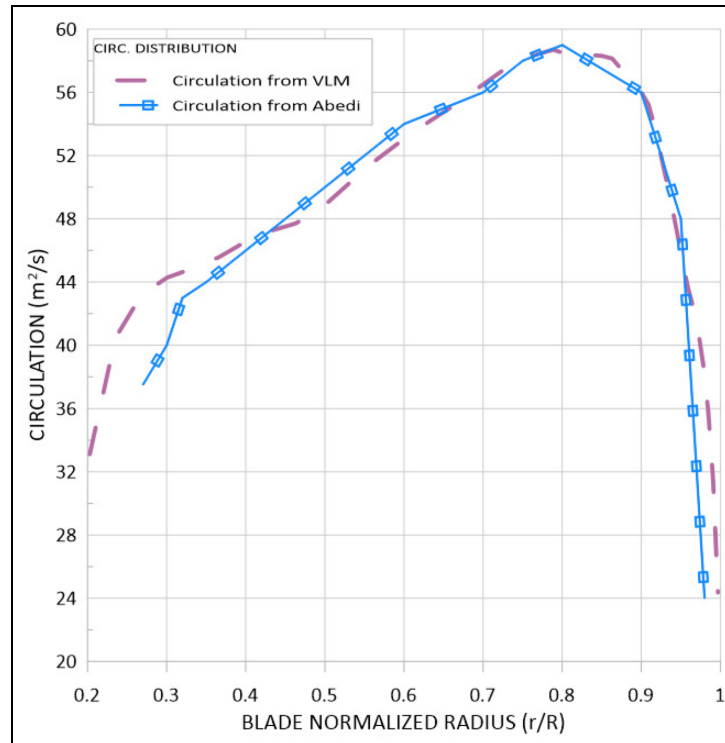


Figure 5. Circulation distribution plotted against blade normalized radius. Results from the implemented VLM are compared to Abedi et al. (2013).

Table 2. Annual operating expense for the NREL 5 MW reference turbine.

Component	Cost (2002 dollars)	Cost (2016 dollars)
O&M costs	\$152,445	\$204,276
Land & lease cost	\$23,520	\$31,517
Levelized replacement cost	\$53,500	\$71,690

Table 3. Levelized cost of energy for the NREL 5 MW wind turbine.

Component	Cost
Initial cost per year (I_c) ←	\$422,389
Annual operating expenses (M_t) ←	\$307,483
Annual energy output (E_t) ←	21,777,132 kWh
Levelized cost of energy (LCOE)	\$ 0.0335/kWh

25 feet in Wichita. The shape and scale factors are scaled to a hub height of 90 m (hub height of the NREL 5 MW reference turbine) using the method presented in Justus and Mikhail (1976). To calculate the power curve for the NREL 5 MW reference turbine, the approximate cubic power curve method is used (Carrillo et al. (2013)). Electrical generator efficiency is set at 94.4% (Jonkman et al. (2009)). The LCOE computed for the NREL 5 MW turbine is presented in Table 3. Again, the objective of the cost model is not to come up with an authoritative cost estimate for the NREL 5 MW. Rather, it is to have a baseline cost for comparison.

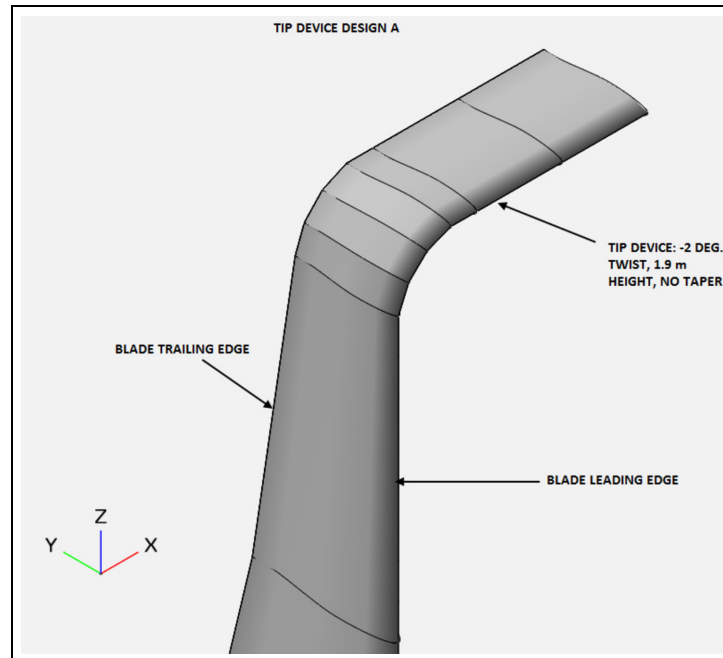


Figure 6. Visual representation of blade tip device Design A.

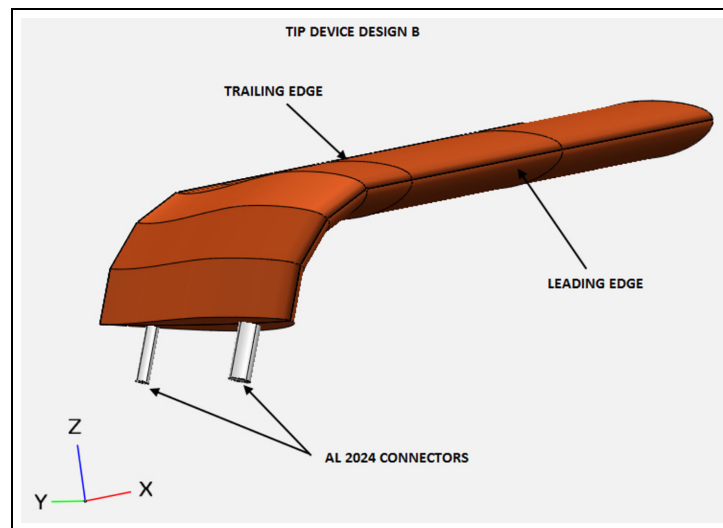


Figure 7. Visual representation of blade tip device Design B.

Blade tip device design

As stated previously, the authors have refrained from calling these blade tip devices winglets. Unlike winglets, which are designed to maximize any increase in C_p by maximizing aerodynamic benefit, these blade tip devices are rather designed to offer an acceptable increase in C_p while keeping the increase in blade bending moments to a minimum. The design philosophy adopted here is to define blade tip devices which, while balancing the generated normal aerodynamic force, centrifugal force, and weight to within a threshold, offer an increase in C_p . A major concern is to minimize root moments.

For the design process, the inflow wind speed and tip speed ratio used is 8 m/s and 7.55 respectively. These conditions lead to peak C_p on the NREL 5 MW turbine. The normal component of lift and centrifugal force are

always directed in opposite directions throughout the blade's revolution. It is thus essential to maintain the weight of the blade tip device at a reasonable minimum. Gaunaa and Johansen (2008) as well as Johansen and Sørensen (2006) show that deflecting winglets to the suction side has greater aerodynamic efficiency, and ensures the wind turbine will not be operating in the wake shed by the winglet. Accordingly, all blade tip devices in this study are deflected to the suction side.

Six parameters are generally considered in the design process for winglets. These parameters are considered here for the blade tip device as well:

1. Airfoil
2. Height
3. Taper ratio
4. Twist
5. Cant angle
6. Sweep.

For this initial study, the effects of airfoil and sweep are not investigated. The airfoil used for the blade tip device is the same as the airfoil in the final blade section of the NREL 5 MW reference turbine.

To find optimum height and taper ratio, the blade tip devices are evaluated at 0° twist and 0° cant angle with varying height and taper ratios. The baseline NREL 5 MW turbine has a rotor overhang of 5 m, shaft tilt of 5° and precone angle of 2.5° . Jonkman et al. (2009) define the maximum out of plane deflection of the NREL 5 MW turbine as 5.5 m. Considering the rotor overhang, shaft tilt, and precone angle, this case leaves a minimum tower clearance of 5.148 m. To prevent tower strikes, a conservative approach is adopted and the maximum height of the blade tip device is restricted to half the tower clearance at the maximum deflection of the blade noted by Jonkman et al. The sensitivity study showed that the most benefit was obtained in using a blade tip device of height 1.9 m, radius of curvature 0.5 m, and no taper. Twist and cant angles play a key role in adhering to the design philosophy of balancing aerodynamic, centrifugal, and gravitational loads. Prior to determining them, however, the mass of the blade tip device must be estimated. Three designs are developed, each with increasing complexity.

Design A

Design A is a "sleeve" blade tip device—one that can be slipped on to the end of the blade and bonded with no need for an adapter or connector. It is constituted of a foam core and balsa spar. Chopped strand fiberglass mat wetted with resin forms a load-bearing skin, with a gel coat (1.5 mils) providing a smooth finish. Tensile and compressive strengths of the blade tip device are determined using basic strength of material techniques. Keeping in mind the simple nature of the blade tip device, all material used is that which is available locally. A visual representation of Design A is shown in Figure 6.

Price estimates are current as of October 2016 (the date of this study). A conservative manufacturing estimate of 8 hours is used, with an employee's salary set at \$20/hour. For installation, a similar conservative approach is used—assuming that the blade tip device can be installed on all three blades by two technicians in two work days, totaling 32 hours of labor and requiring rental of a service lift. The U.S. Bureau of Labor Statistics sets average hourly salary for a wind turbine technician as \$24.55 as of October 2016. The rental rate for a service lift is not readily available, so this is set the same as the hourly salary for a technician. Mass and price estimates for Design A are presented in Table 4.

Design B

Design B uses the same construction method as Design A, except that mounting on the blade is now done with aluminum connectors. On the base of the blade tip device, two circular female connectors, each of length 25 cm, are embedded at the quarter-chord and three-quarter-chord points. The connector at the quarter-chord point has an outer diameter of 10 cm and an inner diameter of 8 cm. The connector at the three-quarter chord point has an outer diameter of 6 cm and an inner diameter of 5 cm. A visual representation of Design B is shown in Figure 7.

Each blade must now be fitted with two male connectors. The blade tip device is held in place by two 0.75-inch SAE 304 18-8 stainless steel bolts that bolt into the connectors. The bolts are designed to be in double shear. Basic structural analysis, similar to Design A, is performed.

Table 4. Mass and cost estimates for Design A.

Component	Mass/Quantity	Cost
Foamular® 150 Rigid XPS foam	11.03 kg	\$114
Balsa spar	1.48 kg	\$47
E-Glass chopped strand mat	1.73 kg	\$19
Polyester resin	2.92 kg	\$20
Gel coat	0.34 kg	\$5
Labor for manufacture	8 hours	\$160
Cost of 1 tip device	1	\$365
Labor for installation	32 hours	\$786
Rental cost—service Lift	32 hours	\$786
Net mass of one blade tip device	17.5 kg	
Net cost of blade tip devices (3)	\$2627	

Table 5. Mass and cost estimates for Design B.

Component	Mass/Quantity	Cost
Blade tip device design A (1 device)	17.5 kg	\$365
Al 2024	4.86 kg	\$22
Additional labor for manufacture	8 hours	\$80
Labor for installation	36 hours	\$884
Rental cost—service Lift	36 hours	\$884
Net mass of one blade tip device	22.36 kg	
Net cost of blade tip devices (3)	\$3129	

Table 6. Cost estimates for Design C.

Component	Mass/Quantity	Cost
Cost per unit surface area	1 m ²	\$604
Cost for 1 blade tip device	7.56 m ²	\$4567
Labor for installation (2 technicians)	36 hours	\$884
Rental cost—service lift	36 hours	\$884
Net cost of 3 blade tip devices	\$15,149	

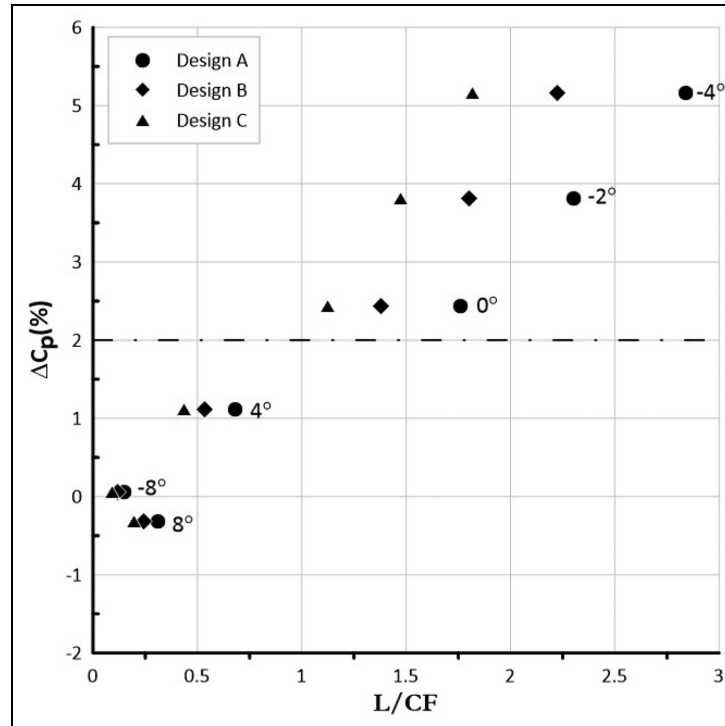
The cost estimate of Design B uses that of Design A, with additional charges to account for the cost of Al 2024 and labor charges for metalwork. Because a standard commodity price for aluminum is not available, the price of aluminum in Wichita as of October 2016 is used, with a conservative margin applied (\$2/lb or \$4.41/kg). Due to the added complexity, an additional 4 hours for manufacture for one blade tip device and an additional 2 hours for installation of all three such devices is allotted. Mass and price estimates for Design B are presented in Table 5.

Design C

Design C serves as a control design. It is simply a tip extension that has been deflected to the suction side and assumes that the blade tip device is constructed in the exact manner as the main blade. A mass estimate is arrived at by using the blade mass density at the last section of the main blade (listed in Jonkman et al., 2009). To arrive at a cost estimate, the cost per unit surface area of the main blade is calculated, and this is multiplied by the surface area of the blade tip device. Labor costs for manufacturing is included in the cost scaling relationship that is used to calculate the cost of the main blade, so it is not necessary to calculate this separately for the blade tip device. Installation costs are considered the same as those of Design B. Cost and mass estimates for Design C are presented in Tables 6 and 7 respectively.

Table 7. Mass estimates for Design C.

Mass per unit length	Tip device length	Total mass
10.32 kg	2.64 m	27.34 kg

**Figure 8.** Percent change in C_p plotted against the ratio of normal aerodynamic to centrifugal force for various twist angles for all three designs.

Blade tip twist

Having arrived at mass estimates, it is now possible to determine the twist angle that allows meaningful improvement in C_p while keeping forces balanced. As mentioned previously, blade tip devices are tested at an inflow speed of 8 m/s and a rotational speed of $\Omega = .9587$ rad/s. Jonkman et al. (2009) note that the NREL 5 MW reference turbine exhibits maximum C_p at these conditions. Various twist angles are tested, and for each twist angle, the ratio of normal aerodynamic force to centrifugal force (L/CF) on the blade tip is calculated. The improvement in C_p is plotted against the ratio of forces for each design. The cant angle throughout this set of iterations is maintained at 90° (i.e. perpendicular to the main blade).

Results

Blade tip device configuration

The improvement in C_p is plotted against the ratio of forces (normal aerodynamic force/centrifugal force, denoted as L/CF) for designs A, B, and C in Figure 8, with the twist angles of the blade tip devices marked. The sign convention adopted in Jonkman et al. (2009) is maintained. Unless the ratio of aerodynamic force to centrifugal force is between 1 and 2.5, the blade tip device is disregarded. Values that are <1 indicate that the blade tip device is too heavy, while larger values indicate the need to ballast the device. A value of 1.5 is selected, because it leaves a margin for fluctuating centrifugal and aerodynamic force throughout the range of operation of the turbine. Additionally, a threshold improvement of $2\%\Delta C_p$ is established, below which the blade tip device is disregarded.

Table 8. Final blade tip device characteristics.

Characteristic	Value
Twist	0°
Taper ratio	1
Height	1.9 m
Radius of curvature	0.5 m

Table 9. Ratio of normal aerodynamic to centrifugal force throughout the operational envelope of the NREL 5 MW wind turbine.

v_∞ (m/s)	Ω (rad/s)	L/CF
3.1	0.838	1.24
8	0.958	1.76
11.4	1.267	1.78
18	1.267	0.94
25	1.267	0.65

even if the forces are perfectly balanced. Although this number is arbitrary, it is a conservative one, and should account for imperfections in the model, such as a prescribed wake and increased roughness due to blade soiling.

As is seen in the plots, only three twist settings offer an improvement in C_p that is above the threshold value. A twist setting of -4° offers the highest improvement in C_p across all three designs, but the ratio of normal aerodynamic force to centrifugal force is not close to balanced. Although a twist setting of -2° offers an increase in C_p , it requires ballast when used with Design A to balance generated centrifugal and normal aerodynamic loads. Using a 0° twist setting does not offer the most improvement in C_p (2.45%). However, because the ratio of forces is at 1.76 for Design A and 1.38 for Design B, it implies minimal need for ballast or reinforcement. This is the final selected configuration. The final characteristics of the selected blade tip devices are presented in Table 8. These blade tip devices offer a meaningful increase in C_p of 2.45% while ensuring normal aerodynamic and centrifugal forces are balanced to within a threshold. The effect of airfoil, sweep, and turbulence intensity have not been measured in this initial study.

For this configuration, the variation in the ratio of normal aerodynamic force to centrifugal force at operational conditions close to cut-in, cut-off, rated, and two intermediate points are presented in Table 9. As expected, the ratio of forces peaks at rated conditions.

Effect on circulation, thrust, and bending moments

The use of blade tip devices leads to a decrease in shed vorticity across the span of the blade, pushing up the circulation distribution. The change in circulation due to the use of blade tip devices is shown in Figure 9. Circulation is higher and circulation gradients are smaller in the tip region with blade tip devices as compared to the baseline blade. This is expected, because the addition of blade tip devices leads to the displacement and diffusion of the tip vortex. The resulting decrease in induced drag and shed vorticity leads to an increase in power produced. Although aerodynamic loading on the blade does extend to the blade tip device, the balancing by centrifugal forces ensures that the tip devices are not highly loaded like traditional winglets.

Reduction in tip effects and an increase in circulation are desirable, but they do lead to an increase in thrust produced by the wind turbine. The increase in thrust and flapwise bending moment due to the application of blade tip devices as described in this study are shown in Table 10. Also shown are bending moments calculated at 90% radius of the blade, the point of attachment of the blade tip. This is calculated for the blade azimuth at 0° , with weight of the blade tip acting along the normal aerodynamic force, thus representing the maximum flapwise bending moment. As is seen, balancing normal aerodynamic load and centrifugal load, and the use of a lightweight blade tip device only leads to a minimal increase in flapwise bending moments at the 90% radius station of the blade.

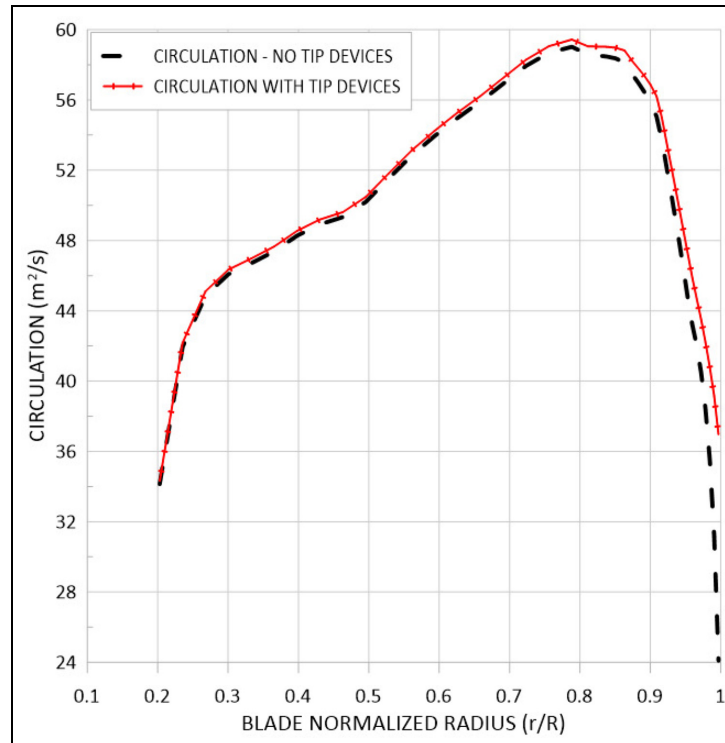


Figure 9. Change in circulation with the addition of blade tip devices.

Table 10. Changes in rotor thrust and flapwise bending moment with the addition of blade tips (BT). Results are for $V_\infty = 8$ m/s and $TSR = 7.55$. Thrust is total rotor thrust, while flapwise BM is for one blade.

	Without BT	With BT	Change (%)
Thrust (kN)	384.54	388.48	1.03
Root BM (kN-m)	5498.77	5581.39	1.5
Added BM at 0.9 r/R (kN-m)	-	0.833	-

Change in annual energy production

At test conditions (inflow speed of 8 m/s and rotational speed of $\Omega = .9587$ rad/s), the improvement in C_p with blade tip devices is calculated to be 2.45%. Using the approximate cubic power curve method in Carrillo et al. (2013) assumes similar performance benefit at all wind speeds. For an NREL 5 MW turbine situated in Wichita, the use of blade tip devices using the proposed design philosophy led to a 1.69% increase in AEP as compared to the baseline case. To determine a monetary value, the average cost per unit of electricity is set at \$ 0.1083/kWh (average cost per unit of electricity in August 2016 as per the U.S. Energy Information Administration). The change in annual energy production due to the use of blade tip devices (described in Table 8) is shown in Table 11. The revenue increase is roughly \$40,000 per machine annually. Change in LCOE for all blade tip device designs are shown in Table 12. All price data was collected using 2016 dollars. However, similar margins can be expected when converting to 2022 dollars. The Bureau of Labor Statistics Consumer Price Index (US Bureau of Labor Statistics, 2022) indicates that \$1 in October 2016 is worth \$1.17 in February 2022. This translates to a revenue increase per machine of roughly \$46,800.

Conclusions

This study provides a proof of concept for retrofit blade tip devices designed with a unique design philosophy. The blade tip devices provide an increase in power production with minimal structural penalty. This increase in power production is accomplished by ensuring that normal aerodynamic and centrifugal loads remain as close to

Table 11. Change in annual energy production (AEP) with and without blade tip devices.

Property	Baseline	With tip devices	Percentage change
Maximum C_p	0.5134	0.5260	2.45
AEP	21,777.14 MWh	22,146.90 MWh	1.69
Increase in revenue (at \$ 0.1083/kWh)	-	-	\$40,046

Table 12. Change in LCOE for all blade tip device designs.

Design	Net profit per year	New LCOE
Design A	\$37,419	\$ 0.03307/kWh
Design B	\$36,917	\$ 0.03309/kWh
Design C	\$24,577	\$ 0.03365/kWh

balanced as possible. By ensuring loads are balanced, a significant increases in flapwise bending moment at the root and at the point of attachment is avoided. The result is a light, cheap blade tip device that does not require the main blade to be structurally reinforced to support it and is economically profitable. Changes in the AEP and the associated changes in LCOE have been captured using an economic model. The use of blade tip devices designed with the proposed design philosophy led to a 2.45% increase in C_p and a 1.69% increase in AEP.

The presented results are the first stage in showing that retrofit blade tip devices developed using the proposed design philosophy are a feasible proposition. Several steps are needed to build on these findings. Only steady state loads were considered in this study. Validating these results with unsteady codes that include atmospheric turbulence is a logical next step. The impact of extreme loads as per IEC standards (Commission, 2005) will also need to be studied. A parametric approach was used here to arrive at the final blade tip device design. An optimization process with more design variables considered and balanced loads as a constraint may lead to tip devices that offer even greater increases in power production while being load neutral. It is also recommended to include the increase in thrust as a design constraint in addition to the forces on the blade tip being balanced. Finally, atmospheric tests with blade tip devices on an operational turbine would establish the validity of the design philosophy.

Acknowledgement

L. Scott Miller, Professor Emeritus in Aerospace Engineering at Wichita State University, was instrumental in conceptualization, and provided guidance, feedback, and mentoring to Vijay Matheswaran. This work was authored in part by the National Renewable Energy Laboratory, operated by Alliance for Sustainable Energy, LLC, for the U.S. Department of Energy (DOE) under Contract No. DE-AC36-08GO28308. Funding provided by the U.S. Department of Energy Office of Energy Efficiency and Renewable Energy Wind Energy Technologies Office. The views expressed in the article do not necessarily represent the views of the DOE or the U.S. Government. The U.S. Government retains and the publisher, by accepting the article for publication, acknowledges that the U.S. Government retains a nonexclusive, paid-up, irrevocable, worldwide license to publish or reproduce the published form of this work, or allow others to do so, for U.S. Government purposes.


Declaration of conflicting interests

The author(s) declared no potential conflicts of interest with respect to the research, authorship, and/or publication of this article.

Funding

The author(s) received no financial support for the research, authorship, and/or publication of this article.

ORCID iD

Vijay Matheswaran  <https://orcid.org/0000-0002-6542-3851>

References

- Abedi H, Davidson L and Voutsinas S (2013) Vortex method application for aerodynamic loads on rotor blades. In: *EWEA 2013: Europe's premier wind energy event*, Vienna, pp.912–921.
- Barlas T, Ramos-García N, Pirrung GR, et al. (2021) Surrogate-based aeroelastic design optimization of tip extensions on a modern 10 MW wind turbine. *Wind Energy Science* 6(2): 491–504.
- Carrillo C, Obando Montano AF, Cidrás J, et al. (2013) Review of power curve modelling for wind turbines. *Renewable and Sustainable Energy Reviews* 21(1): 572–581.
- Commission I (2005) International standard: Wind turbines – Part 1: Design requirements. IEC 61400-1:2005(E), 3 edition.
- Elfarra MA, Sezer-Uzol N and Akmandor IS (2014) Nrel vi rotor blade: Numerical investigation and winglet design and optimization using cfd. *Wind Energy* 17(4): 605–626.
- Fingersh L, Hand M and Laxson A (2006) Wind turbine design cost and scaling model. *NREL/TP-500-40566*. DOI: 10.2172/897434.
- Gaunaa M and Johansen J (2007) Determination of the maximum aerodynamic efficiency of wind turbine rotors with winglets. *Journal of Physics Conference Series* 75: 012006. DOI: 10.1088/1742-6596/75/1/012006.
- Gaunaa M and Johansen J (2008) *Can cp be increased by the use of winglets? – or – a theoretical and numerical investigation of the maximum aerodynamic efficiency of wind turbine rotors with winglets*. AIAA Paper 2008-1314. AIAA Paper 2008-1314. DOI: 10.2514/6.2008-1314.
- Gyatt G and Lissamann P (1985) Development and testing of tip devices for horizontal axis wind turbines. NASA CR-174991.
- Hansen TH and Mühle F (2018) Winglet optimization for a model-scale wind turbine. *Wind Energy* 21(8): 634–649.
- Imamura H, Hasegawa Y and Kikuyama K (1998) Numerical analysis of the horizontal axis wind turbine with winglets. *JSME International Journal* 41(1): 170–176.
- Johansen J, Gaunaa M and Sørensen N (2008) *Increased aerodynamic efficiency of wind turbine rotors using winglets*. AIAA Paper 2008-6728. DOI: 10.2514/6.2008-6728.
- Johansen J and Sørensen N (2006) Aerodynamic investigations of winglets on wind turbine blades using cfd. Risø-R-1543(EN).
- Jong M and Thoman G (1978) Wind characteristics for the western part of Kansas. *WER-4*. DOI: 10.2172/897434.
- Jonkman J, Butterfield S, Musial W, et al. (2009) Definition of a 5-MW reference wind turbine for offshore system development. *NREL/TP-500-38060*. DOI: 10.2172/947422.
- Justus CG and Mikhail A (1976) Height variation of wind speed and wind distributions statistics. *Geophysical Research Letters* 3(5): 261–264.
- Katz J and Plotkin A (eds) (1991) *Low Speed Aerodynamics: From Wing Theory to Panel Methods*, 1st edn. Boca Raton, FL: McGraw-Hill Inc.
- Keckskemety KM and McNamara JJ (2011) Influence of wake effects and inflow turbulence on wind turbine loads. *AIAA Journal* 49(11): 2564–2576.
- Madsen M, Zahle F, Horcas S, et al. (2021) Cfd-based curved tip shape design for wind turbine blades. *Wind Energy Science Discussions*: 1–48. DOI: 10.5194/wes-2021-115.
- Maniaci D and Maughmer M (2012) Winglet design for wind turbines using a free-wake vortex analysis method. AIAA Paper 2012-1158. AIAA Paper 2012-1158. DOI: 10.2514/6.2012-1158.
- Marten D, Wendler J, Pechlivaoglou G, et al. (2013) Qblade: An open source tool for design and simulation of horizontal axis wind turbines. *International Journal of Emerging Technology and Advanced Engineering* 3(3): 264–269.
- Matheswaran V (2016) *Retrofit winglets for wind turbines*. Master's Thesis, Wichita State University, Wichita.
- Matheswaran V, Miller L and Moriarty P (2019) Retrofit winglets for wind turbines. AIAA Paper 2019-1297. DOI: 10.2514/6.2019-1297.
- McDonald R and Gloude-mans J (2022) Open vehicle sketch pad: An open source parametric geometry and analysis tool for conceptual aircraft design. In: *AIAA SCITECH 2022 Forum*. American Institute of Aeronautics and Astronautics. DOI: 10.2514/6.2022-0004.
- Miller L and Matheswaran V (2019) Retrofit winglets for wind turbines. Provisional Patent Application, US Patent and Trademark Office No. 16186876.
- Phillips WF and Snyder DO (2000) Modern adaptation of Prandtl's classic lifting-line theory. *Journal of Aircraft* 37(4): 662–670.
- Schmitz S and Maniaci DC (2017) Methodology to determine a tip-loss factor for highly loaded wind turbines. *AIAA Journal* 55(2): 341–351.
- Tobin N, Hamed A and Chamorro L (2015) An experimental study on the effects of Winglets on the wake and performance of a ModelWind Turbine. *Energies* 8: 11972.
- US Bureau of Labor Statistics (2016) *US Bureau of Labor Statistics, consumer price index inflation calculator*. http://www.bls.gov/data/inflation_calculator.htm (accessed 15 October 2016).
- US Bureau of Labor Statistics (2022) *US Bureau of Labor Statistics, consumer price index inflation calculator*. https://www.bls.gov/data/inflation_calculator.htm (accessed 30 March 2022).
- Van Garrel A (2003) Development of a wind turbine aerodynamics simulation module. *ECN-C-03-079*. DOI: 10.13140/RG.2.1.2773.8000.

- Zahle F, Sørensen NN, McWilliam MK, et al. (2018) Computational fluid dynamics-based surrogate optimization of a wind turbine blade tip extension for maximising energy production. *Journal of Physics Conference Series* 1037(4): 042013. DOI: 10.1088/1742-6596/1037/4/042013
- Zhu B, Sun X, Wang Y, et al. (2017) Performance characteristics of a horizontal axis turbine with fusion winglet. *Energy* 120: 431–440.